EBioMedicine 41 (2019) 244–255

Contents lists available at ScienceDirect

EBioMedicine

journal homepage: www.ebiomedicine.com

EBioMedicine
Published by THE LANCET

A PLK1 kinase inhibitor enhances the chemosensitivity of cisplatin by inducing pyroptosis in oesophageal squamous cell carcinoma

Mengjiao Wu [a], Yan Wang [a], Di Yang [a], Ying Gong [a], Feng Rao [b], Rui Liu [a], Yeerken Danna [a], Jinting Li [a], Jiawen Fan [a], Jie Chen [a], Weimin Zhang [a,*], Qimin Zhan [a,*]

[a] Key laboratory of Carcinogenesis and Translational Research (Ministry of Education/Beijing), Laboratory of Molecular Oncology, Peking University Cancer Hospital & Institute, Beijing 100142, China
[b] Department of Orthopedics and Trauma, Peking University People's Hospital, Beijing, China

ARTICLE INFO

Article history:
Received 2 January 2019
Received in revised form 6 February 2019
Accepted 6 February 2019
Available online 12 March 2019

Keywords:
ESCC
PLK1 inhibitor
Pyroptosis
GSDME
Combination

ABSTRACT

Background: Targeting PLK1 has recently been proven as a viable therapeutic strategy against oesophageal squamous cell carcinom (ESCC). Therefore, this study aimed to explore whether the PLK1 inhibitor BI2536 is able to sensitize ESCC cells to cisplatin (DDP) and determine the underlying mechanisms.
Methods: Viability, clonogenicity, cell cycle distribution and apoptosis were assessed in ESCC cells treated with BI2536 or DDP alone or in combination. Checkpoint activation was examined by immunoblotting and immunohistochemistry. Xenograft model was used to assess the efficacy of the co-treatment. The expression level of GSDME in tissue samples were examined by immunohistochemistry.
Findings: We found that the combination of BI2536 and DDP was synergistic in ESCC cells, which induced pyroptosis in ESCC cells at low doses. Mechanistic studies revealed that BI2536 significantly induced DNA damage and impaired the DNA damage repair pathway in DDP-treated cells both *in vitro* and *in vivo*. Interestingly, we found that co-treatment with BI2536 and DDP induced pyroptosis in ESCC cells depending on the caspase-3/GSDME pathway. Importantly, our study found that GSDME was more highly expressed in tumour tissue than that in normal adjacent tissues, and could serve as a prognostic factor.
Interpretation: BI2536 sensitizes ESCC cells to DDP by inhibiting the DNA damage repair pathway and inducing pyroptosis, which provides new information for understanding pyroptosis. Our study also reveals that the PLK1 inhibitor BI2536 may be an attractive candidate for ESCC targeted therapy, especially when combined with DDP for treating the GSDME overexpression subtype.
Fund: National 973 Program and National Natural Science Fundation of China.

1. Introduction

After surgical treatment and radiotherapy, chemotherapy is the third major treatment for oesophageal squamous cell carcinoma (ESCC) [1,2]. Chemotherapy can cause death in multiple ways in tumour cells, one of which is pyroptosis [3]. However, there are many problems with chemotherapy, such as secondary resistance [4]. Previous studies have shown that tumour cells that are prone to pyroptosis are more sensitive to chemotherapy drugs [3]. This finding suggests that the occurrence of pyroptosis may be an indicator of chemosensitivity.

Pyroptosis, also known as inflammatory cell necrosis, is a new type of programmed cell death discovered and confirmed in recent years [5]. Pyroptosis manifests as cells continue to expand until the cell membrane ruptures, leading to the release of cellular contents and the activation of a strong inflammatory response [6,7]. Pyroptosis is mediated by the gasdermin family [8]. All gasdermins except DFNB59 have a pyroptotic gasdermin-N domain, and the gasdermin-N domain binds membrane lipids and penetrates the membrane [3]. GSDME, also known as DFNA5, is thought to be a tumour suppressor that is cleaved by caspase-3 *in vitro* and causes cell pyroptosis [9,10]. Recent studies have demonstrated that after treating tumour cells with chemotherapeutic drugs *in vitro*, GSDME can be cleaved by caspase-3 to induce pyroptosis in GSDME-expressing tumour cells [3]. The discovery of pyroptosis has attracted widespread attention in the academic community, but the subsequent research has focused mainly on interactions with other proteins, and little is known about the clinical significance of GSDME.

The serine/threonine protein kinase PLK1 plays an important regulatory role in the key steps of mitosis, such as the G2/M transition, maturation of various organelles, and repair of damaged genetic information [11]. PLK1 suppresses the DNA damage response by inactivating the

* Corresponding authors.
E-mail address: qiminzhan@vip.163.com (Q. Zhan).

https://doi.org/10.1016/j.ebiom.2019.02.012

Research in context

Evidence before this study

The gasdermins have been proven as key molecules of the pyroptosis programme. GSDME seemed to be a tumour suppressor gene in recent study. High dosages of chemotherapy drugs could induce caspase-3-mediated pyroptosis in GSDME-positive cell lines.

Added value of this study

Lose-dose cisplatin combined with PLK1 inhibitor BI2536, could induce pyroptosis in GSDME-positive oesophageal squamous cell carcinoma cell lines. The expression of GSDME was significantly higher in tumour tissues than in normal oesophageal tissues. The expression level of GSDME was significantly correlated with a better prognosis in patients with oesophageal squamous cell carcinoma.

Implication of all the available evidence

We therefore propose BI2536 could enhance the chemosensitivity of cisplatin, which could be a candidate as one of the new drug combination strategy for the clinical treatment of oesophageal squamous cell carcinoma. GSDME can be regarded as a promising prognostic marker of oesophageal squamous cell carcinoma. Future investigations in this regard may suggest novel strategies that better harness GSDME-mediated pyroptosis for treatment of cancers.

ATR/Chk1 pathway and the ATM/Chk2 pathway [12,13]. PLK1 gene and protein expression levels are abnormally increased in a variety of tumours, and its expression can be considered an independent negative prognostic marker in many human cancers [14,15]. BI2536 is an ATP-binding domain inhibitor of PLK1 that inhibits the kinase activity of PLK1 at low nanomolar concentrations [16]. BI2536 treatment can induce apoptosis, which is caused by the activation of caspase-3 [17]. PLK1 can directly phosphorylate pro-caspase-8 at S305, which inhibits its processing upon Fas stimulation. When PLK1 is suppressed, pro-caspase-8 is processed and activates caspase-3, which in turn leads to apoptosis [18,19]. However, existing BI2536 clinical trials have revealed serious side effects, such as nausea and severe haematologic toxicity, in patients after treatment [20–22].

Therefore, we suspect that in tumour cells expressing high-level GSDME, combined treatment with BI2536 and the chemotherapy drug cisplatin can increase chemosensitivity. In this study, we demonstrated for the first time that low doses of the PLK1 inhibitor BI2536 combined with cisplatin can increase chemosensitivity by inducing pyroptosis in ESCC *in vivo* and *in vitro*, and these effects were dependent on the BAX/caspase-3/GSDME pathway. Importantly, we also observed that GSDME was overexpressed in a subset of ESCC patients and could serve as a prognostic factor. These findings raised the possibility that synergistically targeting PLK1 with DDP might be a promising strategy for ESCC treatment and that GSDME might serve as a molecular marker for these regimens.

2. Materials and methods

2.1. Cell lines, cell culture and reagent treatment

The human oesophageal squamous cell carcinoma cell lines YES2, KYSE30, KYSE70, KYSE140, KYSE150, KYSE180, KYSE410, KYSE450 and KYSE510 were kindly provided by Dr. Y. Shimada (Kyoto University). These cells were cultured in RPMI 1640 (Lonza, Switzerland) supplemented with 10% foetal bovine serum (Gibco, America) and 1% penicillin/streptomycin (Gibco, America). Both types of ESCC cells were maintained at 37 °C and 5% CO2.

The PLK1 inhibitor BI2536 and DDP were purchased from Selleck (America). For the *in vitro* studies, BI2536 and DDP were prepared as 10 mmol/L stock solutions and stored at −20 °C. BI2536 diluted in culture medium (20 nmol/L) and DDP diluted in culture medium (10 μmol/L) were prepared immediately before use.

2.2. Cell proliferation assay and drug combination studies

The proliferation ability of different tumour cells was detected by MTS assays (Promega) according to the manufacturer's instructions. The data were analysed with GraphPad Prism 5 software and are presented as the percent (%) cell viability relative to the control.

The effects of the drug combination were calculated for each experimental condition using the combination index (CI) method (CalcuSyn software) according to the median-effect analysis of Chou and Talalay [23]. $CI > 1$ indicates antagonism, $CI = 1$ indicates an additive effect, and $CI < 1$ indicates synergy.

2.3. Antibodies

The antibodies used included cleaved-PARP (#5625), Bcl-2 (#3498), MCL-1 (#39224), caspase-8 (#9746), caspase-9 (#9502), Beclin 1 (#3738), P62 (#23214), LC3 A/B (#4108), phospho-Histono H3 (Ser10, #53348), PLK1 (#4513), phospho-PLK1 (Thr210, #9062), phospho-CDC25C (Ser216, #4901), CDC2 (#28439), phospho-CDC2 (Tyr15, #4539), WEE1 (#13084), phospho-WEE1 (Ser642, #4910), caspase-3 (#9665), cleaved caspase-3 (#9661),γH2AX (Ser139; #2577), phospho-BRCA1 (Ser1524, #9009), phospho-ATR (Ser428, #2853), E-cadherin (#14472), Ki-67 (#9027) and GAPDH (#51332), all of which were purchased from Cell Signaling Cytochrome C (ab13575), GSMDE (ab215191), CDC25C (ab32444), GSDMD (ab219800), TOPBP1 (ab2402), RAD51 (ab133534) and 53BP1 (ab36823) antibodies were purchased from Abcam (United Kingdom).

2.4. Flow cytometry analysis

An Annexin V-FITC early apoptosis detection kit (Neobioscience, China) was used to identify apoptotic cells. ESCC cells were treated with BI2536 or cisplatin alone or in combination for 24 h at 37 °C. Approximately 3×10^5 cells were harvested, washed with cold PBS and resuspended in 200 μL of 1× binding buffer. Five microliters of Annexin V-FITC and 5 μL of propidium iodide (PI) were added. After 15 min of incubation at room temperature in the dark, the samples were diluted to a final volume of 400 μL/assay with ice cold 1× binding buffer. Finally, all the samples were analysed by FACS (BD Bioscience, America).

2.5. Colony formation assay

ESCC cells were seeded in 6-well plates at a density of 5000 cells per well. These cells were cultured in RPMI 1640 supplemented with 10% foetal bovine serum and 1% penicillin/streptomycin with the different drug combinations. After two weeks, the cultures were washed with pre-cooled PBS, fixed with methanol and stained with a 0.1% crystal violet solution for 30 min. The colonies were examined and calculated automatically by Image-Pro Plus.

2.6. Cell cycle assay

After treatment with BI2536, DDP or their combination for 24 h, 1×10^6 cells were collected, trypsinized, and fixed in 70% ethanol overnight. Then, the cells were washed three times with pre-cooled PBS and incubated with a PI-staining solution with RNase A (BD Biosciences,

America) for at least 15 min at room temperature before analysis. The cells were run on a FACScan cytometer (BD Biosciences, America) in accordance with the manufacturer's guidelines.

2.7. Microscopy assay

To examine the morphology of apoptotic and pyroptotic cells, cells were seeded in 6-well plates at approximately 30% confluence and subjected to the indicated treatments. Static bright-field cell images were visualized using a Leica microscope.

2.8. Western blot assay

After treatment with clinically relevant doses of BI2536 (20 nmol/L) or DDP (10 μmol/L) alone or in combination for 24 h, cells were harvested in RIPA buffer (Beyotime, China). A total of 20 μg of cellular protein was subjected to 10%–15% SDS-polyacrylamide gel electrophoresis and transferred onto a polyvinylidene difluoride membrane. Incubation with antibodies was performed as described previously. The chemiluminescence signals were detected with an Amersham Imager 600 (GE, America).

2.9. Immunofluorescent staining

Cells treated with clinically relevant doses of BI2536 (20 nmol/L) or DDP (10 μmol/L) alone or in combination were placed on glass slides in 6-well plates. Twenty-four hours later, the cells were fixed in 4% paraformaldehyde for 15 min at room temperature, blocked with 2% BSA and then incubated with 0.1% Triton X-100 for 5 min. The cells were incubated with the indicated antibody at 4 °C overnight. The slides were subsequently incubated with an Alexa Fluor 488-labelled or Alexa Fluor 568-labelled secondary antibody (Invitrogen, A-11034, A-11004) in the dark for 2 h at room temperature. Next, the nuclei were detected by staining with 1 mg/mL DAPI (4′,6-diamidino-2-phenylindole). Images were captured and visualized by a confocal microscope (Leica ST2, Leica, Germany).

2.10. Comet assay

Comet assays, or single-cell gel electrophoresis, were used to determine DNA damage. Cells were assessed using a CometAssay kit (Trevigen, MD). ESCC cells were layered over a frosted microscopic slide after 24 h of the indicated drug treatment. The slides were subjected to electrophoresis in TAE buffer, stained with a PI-staining solution (BD Biosciences, America) and visualized by a Leica fluorescence microscope at 10× magnification. CometScore software (TriTek, VA) was used to analyse the damaged cells (%), the Olive moment, the product of the mean tail migration distance and the fraction of total DNA in the tail for a minimum of 100 cells per condition [24].

2.11. Xenograft studies

Five-week-old female BALB/C nude mice were purchased from Vital River Laboratories (Beijing, China). A total of 1×10^6 KYSE150 cells were injected subcutaneously into the right flanks of mice. The mice were maintained and housed under specific pathogen-free conditions. When the tumour volumes reached approximately 100–150 mm^3, the mice were divided randomly into four treatment groups ($n = 6$). BI2536 and DDP were prepared and administered as recommended by the manufacturer (Selleck Chemicals, America). Next, 15 mg/kg BI2536 was injected intravenously twice a week, whereas 5 mg/kg DDP was injected intraperitoneally once a week as both single agents and in combination for 4 weeks. The last group received PBS by intravenous injection as a control. Tumour sizes were measured twice a week, and the tumour volumes were calculated using the following formula: tumour volume = ((length) × (width) × (width))/2. At the end of the study, the mice were sacrificed, and the tumours were carefully dissected and photographed. All animal care and experiments were conducted in accordance with national and institutional policies for animal health and well-being. The mouse experiments were approved by the Peking University Cancer Hospital Animal Care and Use Committee (Approval NO., ECEA 2018–17). All efforts were made to minimize animal suffering.

2.12. Immunohistochemistry

After routine deparaffinization and hydration, mouse tumour tissue specimens from the four different groups were treated with 3% hydrogen peroxide. The tissue sections were incubated in Tris-EDTA buffer (pH 9.0) and boiled in a microwave oven for 10 min for antigen retrieval. After incubation with 10% normal goat serum, the sections were incubated with anti-Ki67, anti-GSDME, anti-γH2AX and anti-caspase-3 antibodies overnight at 4 °C. Then, the cells were washed and stained with a secondary antibody and DAB (Dako REAL EnVision Detection System, Denmark). The immunohistochemical results were assessed independently by two pathologists from the Department of Pathology of Peking University Cancer Hospital. The criteria for scoring GSDME was as follows. The intensity was graded as follows: 0, negative; 1, weak; 2, moderate; 3, strong. The proportion of positive tumour cells was graded: 0, <5%; 1, 5–25%; 2, 26–50%; 3, 51–75%; 4, >75%. The final score was derived from the multiplication of these two primary scores. Final scores of 0–6 were defined as “low expression” (−); scores of 6–12 as “high expression” (+) [25].

2.13. Ethics statement, tissue specimens and clinicopathological characteristics

Tissue microarrays (TMAs) of ESCC specimens were obtained from Shanghai Outdo Biotech Co., Ltd. (SOBC), with the approval of the Institutional Review Board. Detailed clinicopathological characteristics for all specimens are summarized in Table S1. Written informed consent was obtained from all patients prior to the study. The use of the clinical specimens for research purposes was approved by the Peking University Cancer Hospital Institutional Research Ethics Committee (Approval NO., 2018KT71).

2.14. Statistical analysis

All data were obtained from at least three independent experiments and are expressed as the mean ± SEM. Student's *t*-test and one-way ANOVA were used for statistical analysis of the *in vitro* data. The two-way ANOVA test was used for statistical analysis of the *in vivo* data. Comparisons of the different groups were performed with Student's t-test. Overall survival curves were plotted by the Kaplan-Meier method and compared by log-rank test. The relationships between the 5-year survival rate and GSDME expression were tested using the Chi-square test. $P < .05$ was considered statistically significant for all data.

3. Results

3.1. The PLK1 inhibitor BI2536 enhances the efficacy of DDP by inducing pyroptosis in ESCC cells

We first treated nine ESCC cell lines with DDP at concentrations ranging from 2.5 to 100 μM. Cell viability was evaluated by MTS assay at 72 h after treatment (Fig. 1A, Supplementary file: Table S2). KYSE150 and KYSE510 were the cell lines least sensitive to DDP, so we used those two ESCC cell lines for further experiments. Then, we measured the cell viability by MTS assay at 72 h treated with BI2536 (1 nM to 100 μM, Supplementary file: Table S3). To evaluate whether the effects of BI2536 and DDP were synergic, we determined the CI values through the Chou-Talalay method for the cell lines in which the

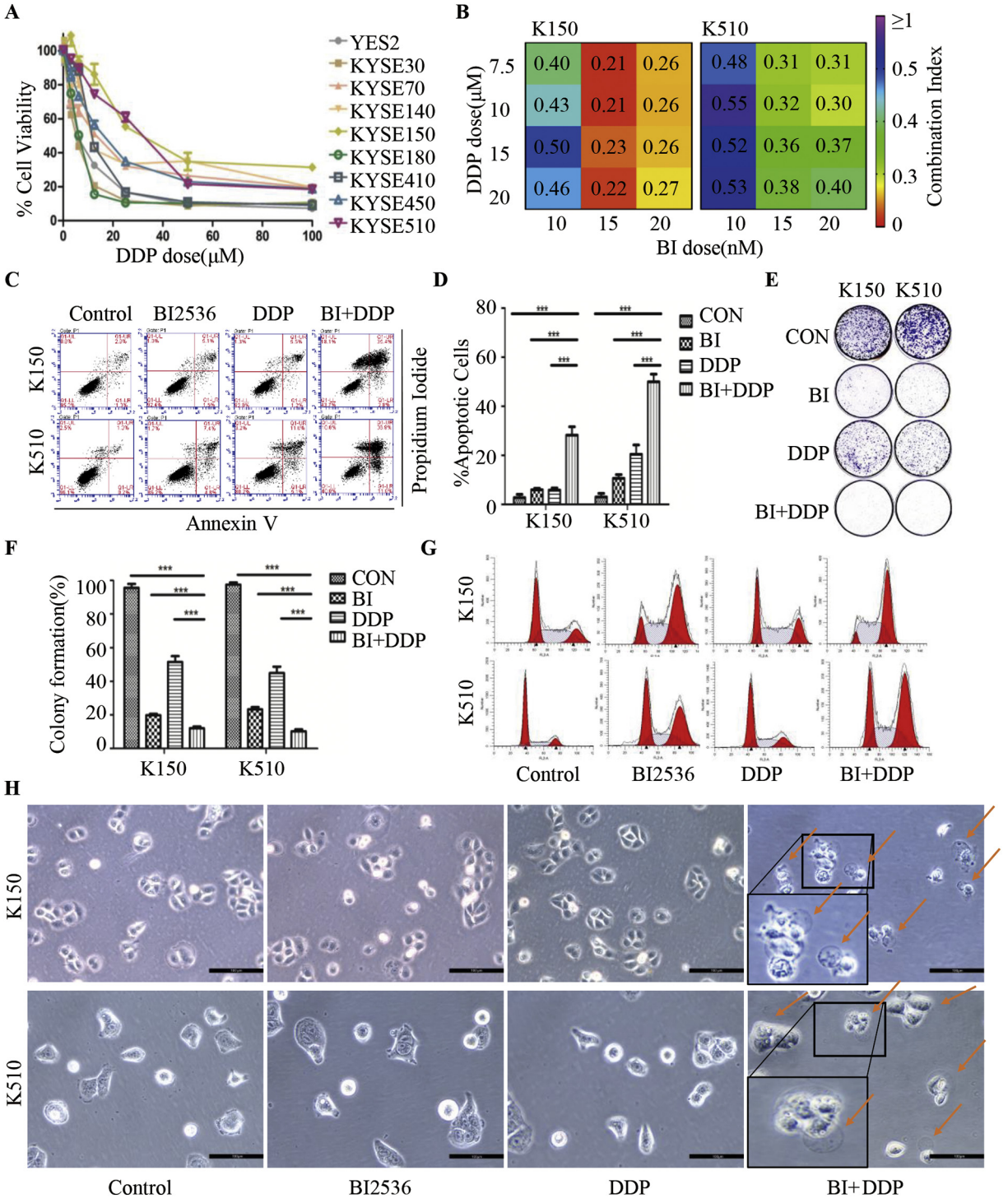

Fig. 1. The PLK1 inhibitor BI2536 enhances the efficacy of DDP by inducing pyroptosis in ESCC cells. (a), Dose-response curves showing the effect of DDP on the viability of 9 different ESCC cell lines. The ESCC cells were seeded in 96-well plates and then treated for 72 h with gradually increasing doses of DDP. Cell viability was assessed using the MTS assay. The IC_{50} of DDP for each cell line was calculated using CalcuSyn software. The results are presented as the mean percentage of viable cells (mean ± SD), averaged from 3 independent experiments, each with 3 replicates per condition. (b), CI heatmaps for KYSE150 (left) and KYSE510 (right) cells treated with the BI2536/DDP combination at the indicated doses of the two drugs for 72 h. The synergy score (CI) was calculated using the equation of Chou and Talay with CalcuSyn. A CI <1.0 indicates synergism. (c), Flow cytometry analysis of annexin V and PI staining of apoptotic cells. ESCC cells were treated with BI2536 (20 nM) or DDP (10 μM) or a combination of both at the same time for 24 h. KYSE150 cells are on the left, and KYSE510 cells are on the right. (d), Quantification of the apoptotic cells is displayed on the right. The results are displayed as the mean ± SEM of three independent experiments. ***, $p < .05$. (e), Results of colony formation assays for KYSE150 (left) and KYSE510 (right) cells. ESCC cells were treated with BI2536 (20 nM) or DDP (10 μM) or a combination of both at the same time for 14 days. (f), The quantification of the cell colonies in E is presented as the mean percentage of viable cells (mean ± SD), averaged from 3 independent experiments, each with 3 replicates per condition. (g), KYSE150 (left) and KYSE510 (right) cells were treated the same as in (c) and subjected to FACS analysis. (h), Representative images of KYSE150 (up) and KYSE510 (below) cells treated with the indicated drugs for 16 h at the doses used in (c). The red arrowheads indicate the characteristic balloons in the cell membrane. The larger image is at the lower left. Original magnification, 200 × .

drug combination was found to be effective. According to the previous study and the aim of reducing drug toxicity [26,27], we treated the two cell lines with the PLK1 inhibitor BI2536 at concentrations ranging from 10 to 20 nM and/or DDP at concentrations ranging from 7.5 to 20 μM for 72 h. The CI values <1 revealed a synergy between the two compounds (Fig. 1B), and these results suggest that BI2536 enhanced the cytotoxic effect of DDP in a low-dose combination.

Both PLK1 inhibitors and DDP have antitumour properties because they induce apoptosis, so we evaluated the effects of these two drugs on apoptosis by cell staining using flow cytometry. Compared with the single drug treatments, co-treatment with BI2536 and DDP for 24 h significantly increased cell apoptosis in both KYSE150 and KYSE510 cell lines (Fig. 1C and D). To explore whether co-treatment with BI2536 and DDP impairs the long-term clonogenic survival of ESCC cells, we performed colony assays for 14 days. Compared to either BI2536 or DDP alone, BI2536 and DDP cooperated to repress the colony formation of ESCC cells (Fig. 1E and F). These results indicated that BI2536 enhances the pro-apoptotic and anti-proliferative efficacy of DDP. Consistently, we found an increase in G2/M arrest in cells treated with BI2536 and DDP in combination compared to that in cells treated with DDP alone after 24 h (Fig. 1G, Supplementary file: Fig. S1A). We found that the expression of molecules upstream and downstream of PLK1 was significantly altered in the group to which BI2536 was added (Supplementary file: Fig. S1B). These results support the hypothesis that ESCC cells treated with BI2536 had impaired cell cycle progression and proliferation.

Notably, after 16 h of co-treatment with BI2536 and DDP, the dying cells became swollen with evident large bubbles extending from the plasma membrane (Fig. 1H), which was a distinct morphological changes characterized as pyroptosis [6]. The proportion of tumour cells under pyroptosis was in the range of 56% to 92% (Supplementary file: Fig. S1C). However, ESCC cells treated with BI2536 or DDP alone did not showed apparent pyroptotic morphological changes. Accordingly, these results indicated that BI2536 enhances the efficacy of DDP by inducing pyroptosis.

3.2. BI2536 and DDP combination treatment leads to caspase-3 activation, which induces pyroptosis by cleaving GSDME in ESCC cells

DDP is a potent apoptotic chemotherapy drug that is effective against many tumours [28]. Given that BI2536 can intensify the pro-apoptotic effect of DDP, we sought to further explore the mechanism of combination therapy. We examined whether BI2536-induced apoptosis in ESCC cells exposed to DDP cytotoxicity is associated with the changes in apoptosis-related proteins, including cleaved-PARP, Bcl-2, BAX, MCL-1 and caspase-8. As expected, we observed a decrease in Bcl-2 family proteins in all ESCC cell lines treated with the two-drug combination compared to cells treated with DDP alone (Fig. 2A). Moreover, the levels of pro-apoptotic proteins, such as cleaved-PARP and cleaved caspase-8, were also increased according to Western blotting (Fig. 2A). These results suggest that BI2536 could indeed increase apoptosis in ESCC cell lines by promoting the caspase-8-mediated activation of the apoptotic pathway and activating PARP, which is a known response to caspase-3 activation. However, other biochemical markers known to cause apoptosis, such as caspase-9, cytochrome C and autophagy, were not significantly affect their protein expression levels (Fig. 2B). These findings suggest that the pro-apoptotic effect of co-treatment with BI2536 and DDP is dependent on the caspase-8-mediated apoptosis pathway but not the mitochondrial apoptotic pathways or autophagy.

The gasdermin-N domains of the gasdermin family give them the ability to form pores. GDMED and GSDME are two proteins of the gasdermin family that have been well studied; both of these proteins work through the gasdermin-N domains [3,8]. However, only GSDME was shown to be cleaved differentially under different treatments (Fig. 2C). Because GSDME is cleaved specifically by activated caspase-3, we examined the activation of caspase-3 by Western blotting. The results showed that the level of cleaved caspase-3 was increased by BI2536 and DDP combination treatment but weakly induced by single agent treatment (Fig. 2C). Next, we sought to determine whether GSDME was essential for pyroptosis induction. We measured the apoptosis-related proteins and gasdermins of the low-expressed GSDME cell line KYSE410 (Supplementary file: Fig. S2A), the results showed that the cleaved caspase-3 and cleaved PARP was increased in the co-treatment group, but there was no cleavage of gasdermins changed (Supplementary file: Fig. S2B). The morphological changes of the death cell in KYSE410 presented nucleus shrinkage, which was special in apoptosis (Supplementary file: Fig. S2C). These findings confirmed that the combination of BI2536 and DDP activated caspase-3 to induce the cleavage of GSDME in GSDME high expressed cell lines and thereby led to pyroptosis.

3.3. BI2536 combined with DDP increases the accumulation of GSDME around the cytoplasm, which induces pyroptosis in ESCC cells

To confirm the ability of BI2536 to increase DDP-induced pyroptosis, we evaluated the co-expression of GSDME and E-cadherin by immunofluorescence. Given E-cadherin is a transmembrane protein of epithelial cells [29], here E-cadherin was served as a membrane marker. Compared to the control and DDP therapy cells groups, KYSE150 and KYSE510 cells treated with BI2536 and DDP for 24 h showed GSDME accumulation in the cytoplasm of those cells undergoing mitosis. We also observed evident cavitation in the cytoplasm of the cells treated with the two drugs together, and GSDME accumulated around the membrane (Fig. 3A and B, Supplementary file: Fig. S3A and Fig. S3B). These results indicate that the accumulation of GSDME is a direct cause of pyroptosis in ESCC cells.

3.4. BI2536 enhances the DNA damage effect of DDP in ESCC cells

To explain how pyroptosis was induced by the co-treatment in ESCC and to confirm that KYSE150 and KYSE510 cells were forced to stop mitosis and leave DNA lesions unrepaired following exposure to BI2536 and DDP, we employed immunofluorescence to analyse the co-expression of γ-H2AX and RAD51, which are markers of DNA double-strand breaks (DSBs) and DNA damage repair (DDR), respectively. We observed a very large fraction of cells that were positive for γ-H2AX staining but negative for RAD51 staining after 24 h of treatment with BI2536 and DDP (Fig. 4A and C, Supplementary file: Fig. S4A and C). These results suggested that BI2536 increased the DNA damage effect of DDP and decreased the DDR ability of ESCC cells. Single-cell gel electrophoresis or comet assays were performed to assess the DNA damage induced by BI2536 and DDP. The results showed that both monotherapy and combination therapy could cause DNA strand breaks, as indicated by the higher frequency of Olive tail moments in the combination group (Fig. 4B and D, Supplementary file: Fig. S4B and D). To assess DNA damage and DDR pathway activation, we performed Western blotting to evaluate the expression of phosphorylated H2AX, TOPBP1, phosphorylated BRCA1, RAD51, 53BP1 and phosphorylated ATR (Fig. 4E). The results showed that the DNA damage marker γH2AX was remarkably increased when cells were treated with both BI2536 and DDP, while this DNA damage marker was hardly detected in the control and single drug groups. These findings indicated that the combination of the two drugs caused significant DNA damage to the ESCC cells. Phosphorylated ATR levels were also increased following the two drug treatments. In contrast, the expression of downstream substrate proteins of phosphorylated ATR, which served as a surrogate marker for DDR pathway activation, was decreased. Consistently, the levels of TOPBP1, phosphorylated BRCA1, RAD51, and 53BP1 were decreased as well. Collectively, these results demonstrated that the combination of BI2536 and DDP inhibited the activation of the DDR pathway.

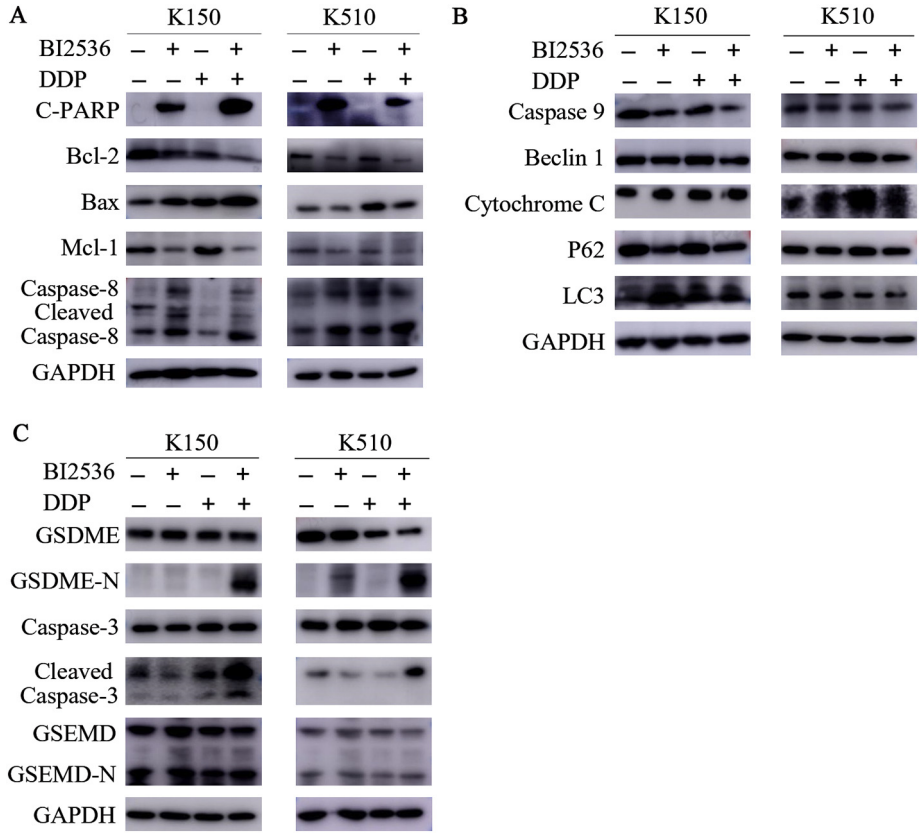

Fig. 2. BI2536 and DDP combination treatment led to caspase-3 activation, which induces pyroptosis by cleaving GSDME in ESCC cells. (a), The expression of several markers that reflect cell apoptosis was examined using Western blotting. Lysates from KYSE150 (left) and KYSE510 (right) cells were probed with antibodies after treatment with BI2536 (20 nM) or DDP (10 μM) or a combination of both at the same time for 24 h. (b), The expression of several markers that reflect the mitochondrial apoptotic pathways or autophagy was examined using Western blotting. Lysates from ESCC cells were probed with antibodies after the same treatment described in (a). (c), The expression of the indicated pyroptosis markers was examined using Western blotting. Lysates from ESCC cells were probed with antibodies after the same treatment described in (a).

3.5. Antitumour efficacy of BI2536 in combination with DDP in a xenograft model

To determine whether the induction of pyroptosis by the combination of BI2526 and DDP suppresses tumour growth *in vivo*, human KYSE150 cells were implanted subcutaneously into the right flanks of immunodeficient BALB/C nude mice. Then, the mouse xenograft models were treated with BI2536 (15 mg/kg) twice a week, DDP (5 mg/kg) once a week, or combination therapy, with PBS as a control. The growth of the tumours treated with combination therapy was significantly slower than that of the tumours treated with BI2536 or DDP alone (Fig. 5A–C). However, body weight loss in the mice treated with combination therapy was not significantly greater than that in the mice treated with DDP alone (Supplementary file: Fig. S5). At the molecular level, the combined treatment induced a higher degree of pyroptosis than the monotherapy in the xenograft model (Fig. 5D). The lowest overall proliferation rate (Ki-67) and the highest levels of DNA damage (γ-H2AX) and apoptosis or pyroptosis (cleaved caspase-3) were also observed in the combination group, further validating the improved anticancer efficiency of BI2536 plus DDP in mice bearing ESCC cells (Fig. 5E). In conclusion, our study revealed that the antitumour efficacy was stronger in the combined treatment group than in the groups treated with BI2536 or DDP alone.

3.6. GSDME is a promising prognostic marker of ESCC

GSDME expression was determined in tissue microarray specimens by immunohistochemical analysis. The tumour samples were obtained from 105 patients with ESCC and from 75 patients with normal oesophageal tissue. GSDME staining was barely detectable in most normal oesophageal tissues, while ESCC tumour tissues exhibited moderate to intense diffuse GSDME staining (Fig. 6A). The staining intensity in normal oesophageal tissues was generally 0–3, while it was typically 3–6 in ESCC tissues (Fig. 6B). The expression of GSDME was significantly higher in ESCC tissues than in normal oesophageal tissues. Interestingly, the expression level of GSDME was significantly correlated with a better prognosis in patients with ESCC ($P < .05$ by the log-rank test, Fig. 6C). Additionally, the 5-year survival rate of the GSDME high expression group was significantly higher than that of the GSDME low expression group (Fig. 6D). The median overall survival among patients with high GSDME expression was 23 months (95% confidence interval, 5 to 100), compared with 15 months (95% confidence interval, 4 to 84) for those with low GSDME expression. These results revealed that GSDME is expressed in a high percentage of ESCC tissues, and it might be a good significant prognostic factor in ESCC patients.

4. Discussion

Platinum-based chemotherapy is the most common therapy for advanced oesophageal cancer, but only 2%–50% of patients have a good response to it [30,31]. Unlike other types of tumours, there has been no significant progress in target therapy for ESCC [32–35]. A recent study showed that targeting cell cycle regulators and the DNA damage response pathway are potential therapeutic strategies for ESCC [36]. In the past studies, overexpression of PLK1 in ESCC was often associated with a poor prognosis because PLK1 inhibits apoptosis and anoikis [15,37]. Considering these findings, we were interested in whether the PLK1 inhibitor BI2536 could sensitize tumour cells to DDP *via* inducing DNA damage. In our study, we found that the PLK1 inhibitor BI2536

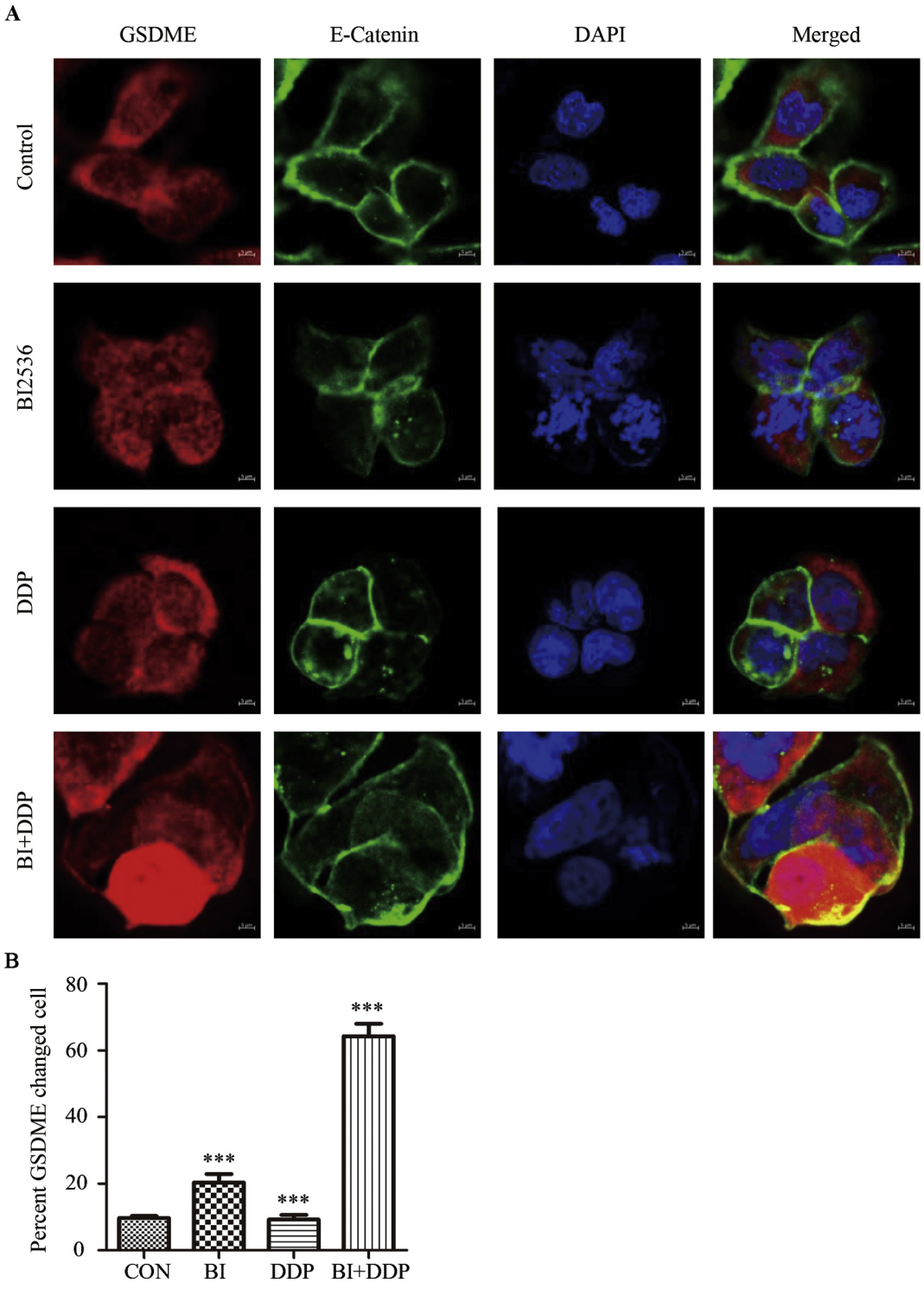

Fig. 3. BI2536 combined with DDP increases the accumulation of GSDME around the cytoplasm, which induces pyroptosis in ESCC cells. (a), Combination treatment was administered to induce cell cycle arrest and GSDME accumulation around the membrane. KYSE510 cells were treated with BI2536 (20 nM), DDP (10 μM), or both for 16 h. Then, the cells were fixed and co-labelled with an anti-GSDME antibody, anti-E-cadherin antibody and DAPI. (b), Quantification of the cells with GSDME changed is displayed. The results are displayed as the mean ± SEM from a minimum of 50 cells per condition of three independent experiments. ***, $p < .05$.

was able to sensitize cells to DDP, thus inducing more DNA damage and pyroptosis to kill the tumour cells. The activation of the BAX/caspase-3/GSDME pathway and the increased DNA damage caused by the inhibition of its repair may be one of the mechanisms underlying the pyroptosis induced by the combination treatment. We also found that GSDME was expressed more highly in ESCC tissues than in normal oesophageal tissues. Analysing GSDME levels in biopsy materials may be used as a prognostic marker for ESCC.

PLK1 is one of the targets of DNA damage checkpoints and is necessary for mitosis reentry after DNA damage checkpoint recovery [38]. Earlier studies suggest that the expression of the gene encoding PLK1 is promoted by Stat3 and NF-κB in ESCC [37,39]. RNA-seq analysis of

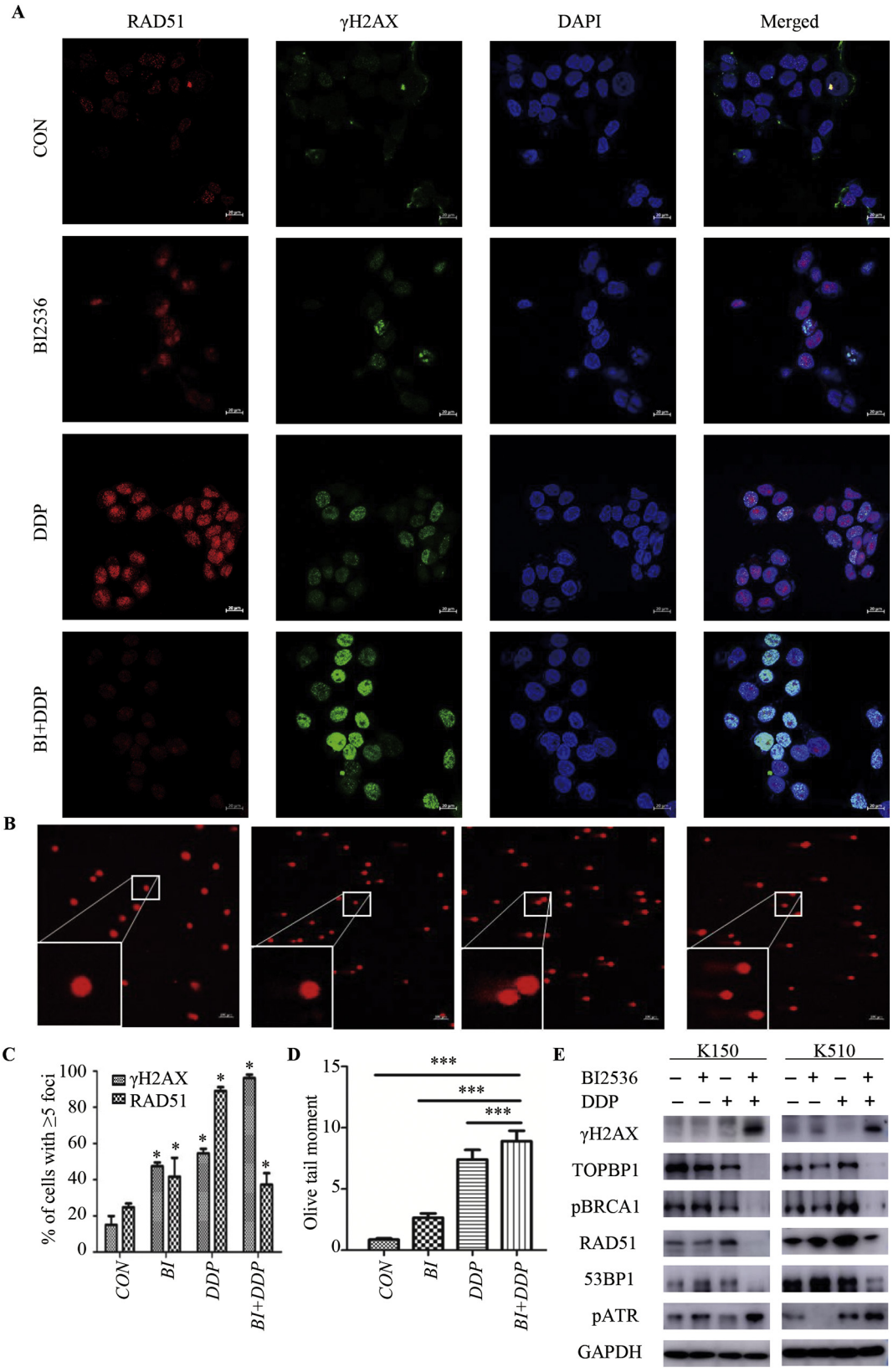

Fig. 4. BI2536 enhances the DNA damage effect of DDP in ESCC cells. (a), KYSE510 cells treated with BI2536 (20 nM), DDP (10 μM), or the combination of the two drugs for 24 h were fixed and co-labelled with anti-γH2AX and anti-RAD51 antibodies and DAPI. The γ-H2AX and RAD51 foci were analysed by immunofluorescence microscopy. (b), KYSE510 cells were treated as described in (a) and analysed *via* comet assay. At the bottom left is the enlarged image. (c), The percentage of cells positive for γ-H2AX and RAD51, which had >5 foci, was calculated. The results are displayed as the mean ± SEM from a minimum of 200 cells per condition for three independent experiments. *, $P < .05$. (d), Olive moment values were normalized to those of KYSE150 cells receiving no treatment. The results are shown as the mean ± SEM from one of three independent experiments. A minimum of 50 cells per experiment were analysed. ***, $P < .05$. (e), The expression of the indicated markers reflecting DNA damage and repair was examined using Western blotting. Lysates from KYSE150 (left) and KYSE510 (right) cells were probed with antibodies after receiving the same treatment described in (a).

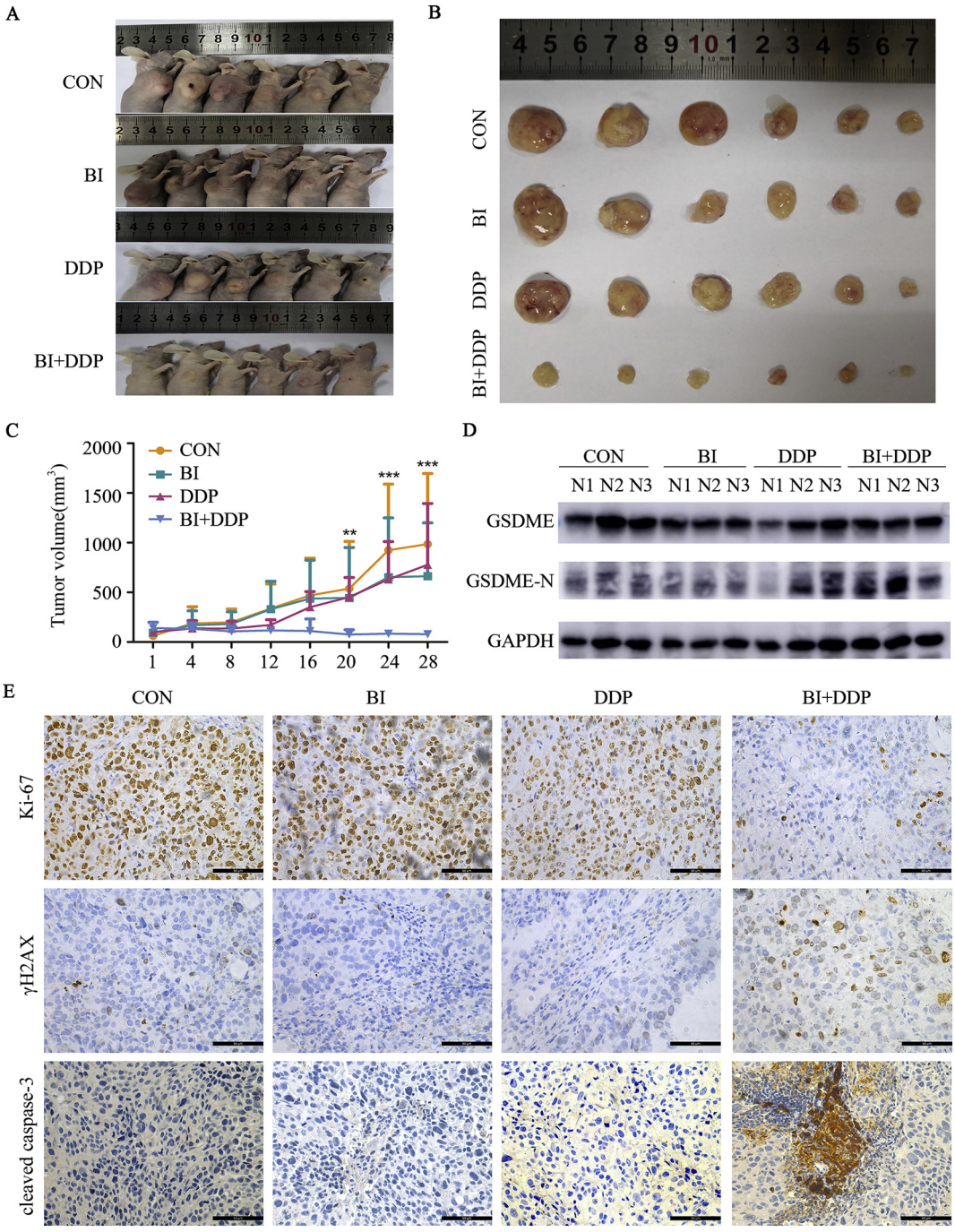

Fig. 5. Antitumour efficacy of BI2536 in combination with DDP in a xenograft model. (a), Tumour sizes in BALB/C nude mice injected subcutaneously with 1×10^6 KYSE150 cells into their right flanks and then injected intravenously with BI2536 (15 mg/kg) or intraperitoneally with DDP (5 mg/kg) or the combination of both drugs. (b), Images of KYSE150-derived xenograft tumours at the end of the study. The mice were sacrificed after 4 weeks of treatment, and tumours were carefully dissected and photographed. (c), Tumour growth curves of the KYSE150-derived mouse xenograft study. The sizes of the tumours in each group were measured twice a week after the onset of treatment ($n = 6$ mice from each experimental group). **, $P < .05$, ***, $P < .001$ compared with the BI2536- or DDP-treated monotherapy group or the untreated group at the end of the study. (d), The expression levels of GSDME and its cleaved N-terminus were examined using Western blotting. The lysates of tumours freshly removed from the bodies were probed with antibodies. (e), Immunohistochemical analyses of Ki-67, γH2AX and cleaved caspase-3 protein expression were performed using tumour sections of KYSE150 mouse xenografts treated as indicated above. Original magnification, 400 × .

mouse embryonic fibroblasts with high expression of PLK1 indicated that PLK1 significantly affected the expression of DDR genes [40]. One previous study showed that receiving monotherapy with another PLK1 inhibitor, B6727, led to DNA damage in small cell lung cancer by activating the ATM/ATR-Chk1/Chk2 checkpoint pathway [41]. Regrettably, several phase II trials showed that receiving monotherapy with BI2536 had limited antitumour activity and dose-limiting side effects in different types of cancers [20,22,42]. Nevertheless, BI2536 exhibited impressive antitumour efficacy when combined with chemotherapy drugs in preclinical studies. In triple-negative breast cancer, BI-2536 increased tumour cell sensitivity to combination chemotherapy with doxorubicin and cyclophosphamide [43]. In malignant peripheral nerve sheath tumours, BI2536 and gemcitabine were highly synergistic [44]. In gastric cancer, BI2536 increased the anti-tumour of DDP in PLK1 overexpressed tumour cell, the Wnt/β-catenin and MEK/ERK/RSK1 signaling pathways changed under the co-treatment [26]. In several research, the researchers compared the sensitization of various PLK1 inhibitions to radiotherapy and chemotherapy, and found that PLK1

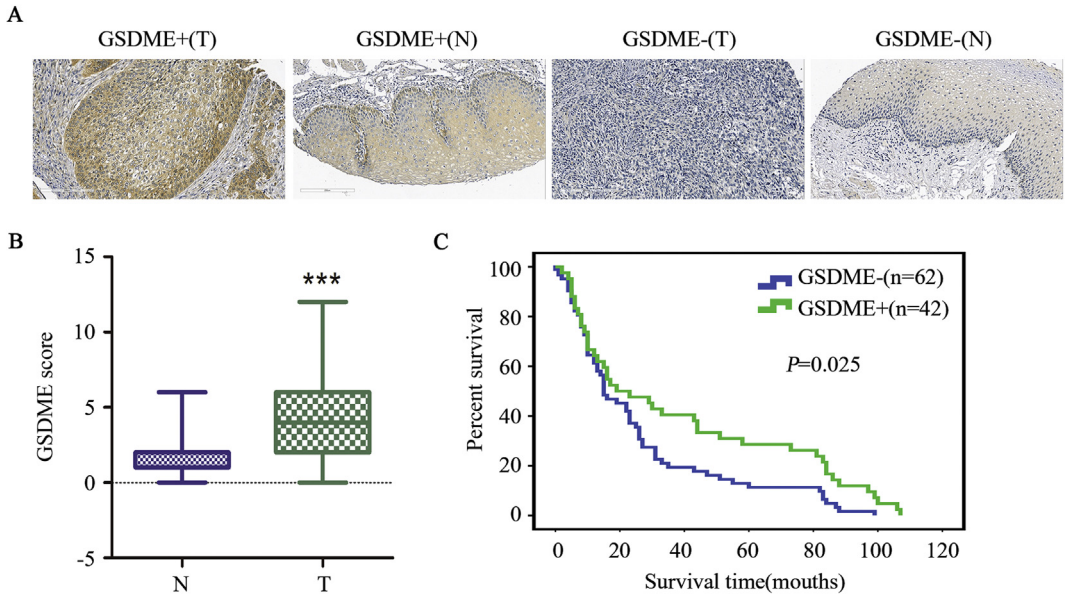

D

	n	GSDME expression		χ^2	*P* value
		High-expression(%)	Low-expression(%)		
<5 years	84	30	54	3.957	0.047
⩾5 years	20	12	8		

Fig. 6. GSDME is a promising prognostic marker of ESCC. (a), GSDME-high (+) and GSDME-low (−) cases of ESCC tissue (T) and normal oesophageal tissue (N) as assessed by immunohistochemistry. (b), GSDME scores were used to evaluate GSDME IHC staining and were calculated for all sample. "T" indicates ESCC tissue samples. "N" indicates normal oesophageal tissue samples. The data are presented as the mean ± SD, ***$P < .05$ compared with normal oesophageal tissue. (c), The difference in survival between patients with high GSDME expression and low GSDME expression was highly significant, as shown by a Kaplan-Meier survival curve ($P < .05$, log-rank test). The median survival time of patients with high GSDME expression was significantly longer than that of patients with low GSDME expression. (d), The difference in the 5-year survival rate between patients with high GSDME expression and low GSDME expression was highly significant.

combined with radiotherapy had a better synergistic effect in Medulloblastoma, Merkel cell carcinoma and bladder carcinoma [27,45,46]. Our study is the first to confirm that inhibiting PLK1 could enhance the chemosensitivity of ESCC cells to DDP. The synergy of these two drugs has been demonstrated *in vitro*, and their strong anticancer efficiency has been confirmed *in vivo*. The mice in the combination group did not lose more weight than the DDP group. Our study could provide a new drug approach for the clinical treatment of ESCC.

The apoptosis induced by the combination treatment of BI2536 and DDP, however, is multi-factorial and complex. This co-treatment prevents ESCC cells that have suffered DNA damage from repairing themselves and forces those cells to have a different fate at the time they face cell death. There is no doubt that cells with high GSDME expression switch apoptosis to pyroptosis *via* caspase-3 [9]. It has been proven that a high dosage of chemotherapy drugs, such as topotecan, etoposide and DDP, could induce caspase-3-mediated apoptosis in GSDME-positive cell lines [3]. However, in our study, no significant pyroptosis was observed in the DDP group because the dose of DDP as a single agent was too weak to induce caspase-3 activity. Thus, it was reasonable to speculate that the combination of BI2536 and DDP induced pyroptosis. In addition, we observed morphological changes and protein levels characteristic of pyroptosis in ESCC cells before apoptosis. We also observed that inhibiting PLK1 induced the upregulation and accumulation of GSDME surrounding the membrane in mitotic cells. Small amounts of the cleaved GSDME N-terminal were also observed in the BI2536 group. This finding led us to suspect that the inhibition of PLK1 might alter the metabolic pathways of GSDME in cells, and PLK1 inhibitor monotherapy at a high dosage could also induce pyroptosis. However, the serious dose-limiting side effects of BI2536 in several phase II trials prevented us from further research. The PLK1 inhibitor arrested more cells at the G2/M phase [38], while GSDME executed its pore-forming function *via* activated caspase-3 [3]. These findings may explain why cells with high GSDME expression choose pyroptosis. There was still a portion of the cells executing apoptosis under the combined treatment. DNA damage induced by BI2536 and DDP activated the downstream apoptotic pathway. In our study, caspase-8 was apparently cleaved and activated. The caspase-8-dependent proteolytic maturation of the activated caspase-3 is sufficient to induce regulated cell death [47]. We further showed that most apoptosis in our research was caspase-8-mediated extrinsic apoptosis instead of intrinsic apoptosis. In a recent study, a PLK1 inhibitor promoted autophagy [48,49]. However, in our study, we did not observe significant changes in autophagy markers in any group. These results may indicate that autophagy is not the primary reason for the antitumour activity of the combined treatment in our study.

The gasdermin family has been identified as key molecules of the pyroptosis programme. GSDME first attracted the attention of investigators as a hearing impairment gene in 1995 [50]. Three years later, Thompson and Weigel found that the expression pattern of GSDME was inversely correlated with oestrogen receptor (ER) expression in primary breast cancer. This was the first time that GSDME had been reported to be related to tumours [51]. Melanoma cell lines with negative GSDME expression showed resistance to etoposide, but transfecting an expression vector encoding GSDME increased the sensitivity to etoposide [52]. In primary gastric cancer and colorectal cancer, GSDME can be suppressed by methylation [53,54]. GSDME was also methylated in ER-positive breast cancer and was found to be associated with lymph node metastasis [55]. Thus, GSDME appeared to be a tumour suppressor. No differences have been found in the activation of caspase-3 by intrinsic or extrinsic apoptotic pathways, and these pathways all induced GSDME cleavage in cancer cells [56]. There have been more research advances in GSDMD in pyroptosis over the past years [7]. GSDMD was proven to be the substrate of inflammasome-associated caspases, such

as caspase-1 and caspase-11 [57]. In our study, when ESCC cells were treated with both BI2536 and DDP, GSDME, rather than GSDMD, played a role in pyroptosis. GSDMD did not play a crucial role in inducing apoptosis in our study because its cleaved N-terminal domain form was not significantly changed (Fig. 2C). In addition, we discovered that GSDME, which is highly expressed in a subset of ESCC patients, was correlated with better overall survival. This result might indicate that GSDME could be regarded as a new useful prognostic marker for ESCC. In this research, GSDME accumulated and was activated by caspase-3 in the cell lines with high GSDME expression that were treated with the two drugs; ultimately, GSDME exerted its function of inducing pyroptosis. We hypothesized that high GSDME expression could be a good predictor for ESCC treatment. Patients with high GSDME expression might be more sensitive to the combination treatment of PLK1 inhibitor and DDP, and the antitumour effect of these drugs would be better. It is reasonable to speculated that tumour cell with high GSDME expression was vulnerable to suffer pyroptosis when under endogenous or exogenous stresses. To this end, the data on GSDME and PLK1 have revealed a good therapeutic target and prognostic indicator for ESCC. This finding might provide a promising direction for the development of personalized, precision medicine for ESCC in the future.

In sum, our study revealed that the PLK1 inhibitor BI2536 may be an attractive candidate for ESCC treatment, especially when combined with DDP. Our results also reveal new information for understanding pyroptosis induction. Further investigations focusing on the potential antitumour activity of BI2536 and DDP could shed light on the benefit that patients could gain from receiving this well-tolerated chemotherapy regimen and could determine the relevance of GSDME expression to therapeutic effects.

Funding

This work is supported by the National 973 Program (2015CB553904), National Natural Science Fundation of China (81490753, 81830086, 81702748 and 81802780), China Postdoctoral Science Foundation (2017M620010), National Postdoctoral Program for Innovative Talent, Science Foundation of Peking University Cancer Hospital (2017-27), “Beijing Municipal Administration of Hospitals” Mission Plan (SML20181101), the Fundamental Research Funds for the Central Universities(PKU2017RC001), Special Projects for Strengthening Basic Research of Peking University (BMU2018JC006).

Author contributions

M.W., Y.W., D.Y., Y.G., F.R. and J.T. performed experiments. R.L., Y.D. and J.C. helped to analyse and interpreted the data. M.W. and J.F. facilitated IHC result interpretation. M.W., W.Z. and Q.Z. designed the experiments. M.W. and W.Z. wrote and edited the paper. All authors read and approved the final manuscript.

Competing financial interests

No potential conflicts of interest were disclosed.

Acknowledgements

The authors would like to thank Zhihua Tian and Xijuan Liu from Peking University Cancer Hospital and Institute for their technical help about the confocal imaging and the flow cytometry analysis. We would like to thank Dr. Yingwei Ge for discussion of the manuscript.

Appendix A. Supplementary data

Supplementary data to this article can be found online at https://doi.org/10.1016/j.ebiom.2019.02.012.

References

[1] Davies AR, Gossage JA, Zylstra J, Mattsson F, Lagergren J, Maisey N, et al. Tumor stage after neoadjuvant chemotherapy determines survival after surgery for adenocarcinoma of the esophagus and esophagogastric junction. J Clin Oncol 2014;32(27):2983–90.
[2] Zhao Y, Dai Z, Min W, Sui X, Kang H, Zhang Y, et al. Perioperative versus preoperative chemotherapy with surgery in patients with resectable squamous cell carcinoma of esophagus: a phase III randomized trial. J Thorac Oncol 2015;10(9):1349–56.
[3] Wang Y, Gao W, Shi X, Ding J, Liu W, He H, et al. Chemotherapy drugs induce pyroptosis through caspase-3 cleavage of a gasdermin. Nature 2017;547(7661):99–103.
[4] Saraswathy M, Gong S. Different strategies to overcome multidrug resistance in cancer. Biotechnol Adv 2013;31(8):1397–407.
[5] de Gassart A, Martinon F. Pyroptosis: caspase-11 unlocks the gates of death. Immunity 2015;43(5):835–7.
[6] Shi J, Gao W, Shao F. Pyroptosis: gasdermin-mediated programmed necrotic cell death. Trends Biochem Sci 2017;42(4):245–54.
[7] Kayagaki N, Stowe IB, Lee BL, O'Rourke K, Anderson K, Warming S, et al. Caspase-11 cleaves gasdermin D for non-canonical inflammasome signalling. Nature 2015;526(7575):666–71.
[8] He WT, Wan H, Hu L, Chen P, Wang X, Huang Z, et al. Gasdermin D is an executor of pyroptosis and required for interleukin-1beta secretion. Cell Res 2015;25(12):1285–98.
[9] Rogers C, Fernandes-Alnemri T, Mayes L, Alnemri D, Cingolani G, Alnemri ES. Cleavage of DFNA5 by caspase-3 during apoptosis mediates progression to secondary necrotic/pyroptotic cell death. Nat Commun 2017;8:14128.
[10] Masuda Y, Futamura M, Kamino H, Nakamura Y, Kitamura N, Ohnishi S, et al. The potential role of DFNA5, a hearing impairment gene, in p53-mediated cellular response to DNA damage. J Hum Genet 2006;51(8):652–64.
[11] Gutteridge RE, Ndiaye MA, Liu X, Ahmad N. Plk1 inhibitors in cancer therapy: from laboratory to clinics. Mol Cancer Ther 2016;15(7):1427–35.
[12] Mamely I, van Vugt MA, Smits VA, Semple JI, Lemmens B, Perrakis A, et al. Polo-like kinase-1 controls proteasome-dependent degradation of Claspin during checkpoint recovery. Curr Biol 2006;16(19):1950–5.
[13] Li Z, Li J, Kong Y, Yan S, Ahmad N, Liu X. Plk1 phosphorylation of Mre11 antagonizes the DNA damage response. Cancer Res 2017;77(12):3169–80.
[14] Takai N, Hamanaka R, Yoshimatsu J, Miyakawa I. Polo-like kinases (Plks) and cancer. Oncogene 2005;24(2):287–91.
[15] Feng YB, Lin DC, Shi ZZ, Wang XC, Shen XM, Zhang Y, et al. Overexpression of PLK1 is associated with poor survival by inhibiting apoptosis via enhancement of survivin level in esophageal squamous cell carcinoma. Int J Cancer 2009;124(3):578–88.
[16] Steegmaier M, Hoffmann M, Baum A, Lenart P, Petronczki M, Krssak M, et al. BI 2536, a potent and selective inhibitor of polo-like kinase 1, inhibits tumor growth in vivo. Curr Biol 2007;17(4):316–22.
[17] Shin SB, Woo SU, Yim H. Differential cellular effects of Plk1 inhibitors targeting the ATP-binding domain or polo-box domain. J Cell Physiol 2015;230(12):3057–67.
[18] Matthess Y, Raab M, Knecht R, Becker S, Strebhardt K. Sequential Cdk1 and Plk1 phosphorylation of caspase-8 triggers apoptotic cell death during mitosis. Mol Oncol 2014;8(3):596–608.
[19] Jang MS, Lee SJ, Kang NS, Kim E. Cooperative phosphorylation of FADD by Aur-A and Plk1 in response to taxol triggers both apoptotic and necrotic cell death. Cancer Res 2011;71(23):7207–15.
[20] Awad MM, Chu QS, Gandhi L, Stephenson JJ, Govindan R, Bradford DS, et al. An open-label, phase II study of the polo-like kinase-1 (Plk-1) inhibitor, BI 2536, in patients with relapsed small cell lung cancer (SCLC). Lung Cancer (Amsterdam, Netherlands) 2017;104:126–30.
[21] Mross K, Dittrich C, Aulitzky WE, Strumberg D, Schutte J, Schmid RM, et al. A randomised phase II trial of the Polo-like kinase inhibitor BI 2536 in chemo-naive patients with unresectable exocrine adenocarcinoma of the pancreas - a study within the Central European Society Anticancer Drug Research (CESAR) collaborative network. Br J Cancer 2012;107(2):280–6.
[22] Sebastian M, Reck M, Waller CF, Kortsik C, Frickhofen N, Schuler M, et al. The efficacy and safety of BI 2536, a novel Plk-1 inhibitor, in patients with stage IIIB/IV non-small cell lung cancer who had relapsed after, or failed, chemotherapy: results from an open-label, randomized phase II clinical trial. J Thorac Oncol 2010;5(7):1060–7.
[23] Chou TC. Theoretical basis, experimental design, and computerized simulation of synergism and antagonism in drug combination studies. Pharmacol Rev 2006;58(3):621–81.
[24] Duez P, Dehon G, Kumps A, Dubois J. Statistics of the comet assay: a key to discriminate between genotoxic effects. Mutagenesis 2003;18(2):159–66.
[25] Xue L, Ren L, Zou S, Shan L, Liu X, Xie Y, et al. Parameters predicting lymph node metastasis in patients with superficial esophageal squamous cell carcinoma. Mod Pathol 2012;25(10):1364–77.
[26] Lian G, Li L, Shi Y, Jing C, Liu J, Guo X, et al. BI2536, a potent and selective inhibitor of polo-like kinase 1, in combination with cisplatin exerts synergistic effects on gastric cancer cells. Int J Oncol 2018;52(3):804–14.
[27] Brassesco MS, Pezuk JA, Morales AG, de Oliveira JC, Roberto GM, da Silva GN, et al. In vitro targeting of Polo-like kinase 1 in bladder carcinoma: comparative effects of four potent inhibitors. Cancer Biol Ther 2013;14(7):648–57.
[28] Siddik ZH. Cisplatin: mode of cytotoxic action and molecular basis of resistance. Oncogene 2003;22(47):7265–79.
[29] Lecuit T, Yap AS. E-cadherin junctions as active mechanical integrators in tissue dynamics. Nat Cell Biol 2015;17(5):533–9.
[30] Ilson DH, van Hillegersberg R. Management of patients with adenocarcinoma or squamous cancer of the esophagus. Gastroenterology 2018;154(2):437–51.

[31] Abnet CC, Arnold M, Wei WQ. Epidemiology of esophageal squamous cell carcinoma. Gastroenterology 2018;154(2):360–73.
[32] Okines AF, Ashley SE, Cunningham D, Oates J, Turner A, Webb J, et al. Epirubicin, oxaliplatin, and capecitabine with or without panitumumab for advanced esophagogastric cancer: dose-finding study for the prospective multicenter, randomized, phase II/III REAL-3 trial. J Clin Oncol 2010;28(25):3945–50.
[33] Luber B, Deplazes J, Keller G, Walch A, Rauser S, Eichmann M, et al. Biomarker analysis of cetuximab plus oxaliplatin/leucovorin/5-fluorouracil in first-line metastatic gastric and oesophago-gastric junction cancer: results from a phase II trial of the Arbeitsgemeinschaft Internistische Onkologie (AIO). BMC Cancer 2011;11:509.
[34] Bang YJ, Van Cutsem E, Feyereislova A, Chung HC, Shen L, Sawaki A, et al. Trastuzumab in combination with chemotherapy versus chemotherapy alone for treatment of HER2-positive advanced gastric or gastro-oesophageal junction cancer (ToGA): a phase 3, open-label, randomised controlled trial. Lancet (London, England) 2010;376(9742):687–97.
[35] Van Cutsem E, de Haas S, Kang YK, Ohtsu A, Tebbutt NC, Ming Xu J, et al. Bevacizumab in combination with chemotherapy as first-line therapy in advanced gastric cancer: a biomarker evaluation from the AVAGAST randomized phase III trial. J Clin Oncol 2012;30(17):2119–27.
[36] Smyth EC, Lagergren J, Fitzgerald RC, Lordick F, Shah MA, Lagergren P, et al. Oesophageal cancer. Nat Rev Dis Primers 2017;3:17048.
[37] Lin DC, Zhang Y, Pan QJ, Yang H, Shi ZZ, Xie ZH, et al. PLK1 is transcriptionally activated by NF-kappaB during cell detachment and enhances anoikis resistance through inhibiting beta-catenin degradation in esophageal squamous cell carcinoma. Clin Cancer Res 2011;17(13):4285–95.
[38] van Vugt MA, Bras A, Medema RH. Polo-like kinase-1 controls recovery from a G2 DNA damage-induced arrest in mammalian cells. Mol Cell 2004;15(5):799–811.
[39] Zhang Y, Du XL, Wang CJ, Lin DC, Ruan X, Feng YB, et al. Reciprocal activation between PLK1 and Stat3 contributes to survival and proliferation of esophageal cancer cells. Gastroenterology 2012;142(3):521–30 [e3].
[40] Li Z, Liu J, Li J, Kong Y, Sandusky G, Rao X, et al. Polo-like kinase 1 (Plk1) overexpression enhances ionizing radiation-induced cancer formation in mice. J Biol Chem 2017;292(42):17461–72.
[41] Wang Y, Wu L, Yao Y, Lu G, Xu L, Zhou J. Polo-like kinase 1 inhibitor BI 6727 induces DNA damage and exerts strong antitumor activity in small cell lung cancer. Cancer Lett 2018;436:1–9.
[42] Schoffski P, Blay JY, De Greve J, Brain E, Machiels JP, Soria JC, et al. Multicentric parallel phase II trial of the polo-like kinase 1 inhibitor BI 2536 in patients with advanced head and neck cancer, breast cancer, ovarian cancer, soft tissue sarcoma and melanoma. The first protocol of the European Organization for Research and Treatment of Cancer (EORTC) Network Of Core Institutes (NOCI). Eur J Cancer 2010;46(12):2206–15.
[43] Maire V, Nemati F, Richardson M, Vincent-Salomon A, Tesson B, Rigaill G, et al. Polo-like kinase 1: a potential therapeutic option in combination with conventional chemotherapy for the management of patients with triple-negative breast cancer. Cancer Res 2013;73(2):813–23.
[44] Kolberg M, Bruun J, Murumagi A, Mpindi JP, Bergsland CH, Holand M, et al. Drug sensitivity and resistance testing identifies PLK1 inhibitors and gemcitabine as potent drugs for malignant peripheral nerve sheath tumors. Mol Oncol 2017;11(9):1156–71.
[45] Pezuk JA, Brassesco MS, Ramos PMM, Scrideli CA, Tone LG. Polo-like kinase 1 pharmacological inhibition as monotherapy or in combination: comparative effects of polo-like kinase 1 inhibition in medulloblastoma cells. Anticancer Agents Med Chem 2017;17(9):1278–91.
[46] Kadletz L, Bigenzahn J, Thurnher D, Stanisz I, Erovic BM, Schneider S, et al. Evaluation of Polo-like kinase 1 as a potential therapeutic target in Merkel cell carcinoma. Head Neck 2016;38(Suppl. 1):E1918–25.
[47] Barnhart BC, Alappat EC, Peter ME. The CD95 type I/type II model. Semin Immunol 2003;15(3):185–93.
[48] Chan KK, Wong OG, Wong ES, Chan KK, Ip PP, Tse KY, et al. Impact of iASPP on chemoresistance through PLK1 and autophagy in ovarian clear cell carcinoma. Int J Cancer 2018;143(6):1456–69.
[49] Ruf S, Heberle AM, Langelaar-Makkinje M, Gelino S, Wilkinson D, Gerbeth C, et al. PLK1 (polo like kinase 1) inhibits MTOR complex 1 and promotes autophagy. Autophagy 2017;13(3):486–505.
[50] van Camp G, Coucke P, Balemans W, van Velzen D, van de Bilt C, van Laer L, et al. Localization of a gene for non-syndromic hearing loss (DFNA5) to chromosome 7p15. Hum Mol Genet 1995;4(11):2159–63.
[51] Thompson DA, Weigel RJ. Characterization of a gene that is inversely correlated with estrogen receptor expression (ICERE-1) in breast carcinomas. Eur J Biochem 1998;252(1):169–77.
[52] Lage H, Helmbach H, Grottke C, Dietel M, Schadendorf D. DFNA5 (ICERE-1) contributes to acquired etoposide resistance in melanoma cells. FEBS Lett 2001;494(1–2):54–9.
[53] Kim MS, Chang X, Yamashita K, Nagpal JK, Baek JH, Wu G, et al. Aberrant promoter methylation and tumor suppressive activity of the DFNA5 gene in colorectal carcinoma. Oncogene 2008;27(25):3624–34.
[54] Akino K, Toyota M, Suzuki H, Imai T, Maruyama R, Kusano M, et al. Identification of DFNA5 as a target of epigenetic inactivation in gastric cancer. Cancer Sci 2007;98(1):88–95.
[55] Kim MS, Lebron C, Nagpal JK, Chae YK, Chang X, Huang Y, et al. Methylation of the DFNA5 increases risk of lymph node metastasis in human breast cancer. Biochem Biophys Res Commun 2008;370(1):38–43.
[56] Feng S, Fox D, Man SM. Mechanisms of gasdermin family members in inflammasome signaling and cell death [J]. J Mol Biol 2018;430:3068–80 (18 Pt B).
[57] Shi J, Zhao Y, Wang K, Shi X, Wang Y, Huang H, et al. Cleavage of GSDMD by inflammatory caspases determines pyroptotic cell death. Nature 2015;526(7575):660–5.